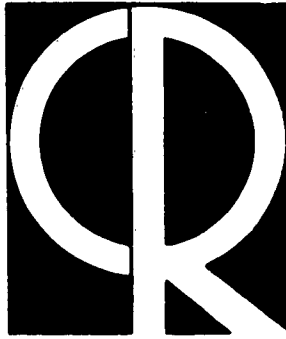


AFCRL-63-57
FEBRUARY 1963

03-3-5

CAMBRIDGE
AFCRL
#03474



Research Report

Microwave Phonon Generation by Thin Magnetic Films

MARDEN H. SEAVEY, JR.

A03 A7A

Requests for additional copies by Agencies of the Department of Defense, their contractors, and other government agencies should be directed to the:

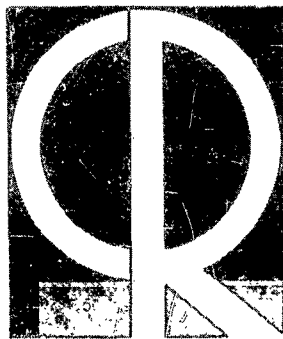
Armed Services Technical Information Agency
Arlington Hall Station
Arlington 12, Virginia

Department of Defense contractors must be established for ASTIA services, or have their 'need-to-know' certified by the cognizant military agency of their project or contract.

All other persons and organizations should apply to the:

U. S. DEPARTMENT OF COMMERCE
OFFICE OF TECHNICAL SERVICES,
WASHINGTON 25, D. C.

AFCRL-63-57
FEBRUARY 1963



Research Report

Microwave Phonon Generation by Thin Magnetic Films

MARDEN H. SEAVEY, JR.

Abstract

The magnetostrictive generation of microwave phonons by thin magnetic films is theoretically described and experimental data taken at X-band are discussed. The cases of generation on the uniform precession on ferromagnetic resonance (FMR) and on spin-wave resonance (SPWR) are treated. Wave equations are obtained for the displacement components when the dc magnetic field makes an arbitrary angle with the film normal. These have driving terms proportional to dm/dy which are responsible for the phonon generation. It is shown that in the FMR case the generation occurs at the film surfaces, while in the SPWR case the generation takes place throughout the film interior. The experimental data appear to support the generation model in the FMR case, but unexplained discrepancies exist between theory and experiment in the SPWR case. A comparison with quartz piezoelectric generation is made, and while the generation efficiencies are about equal, substantial improvement is possible in the magnetostrictive case.

Acknowledgments

The author wishes to acknowledge the collaboration with Dr. P. E. Tannenwald in the initial phases of the work, the support of M. I. T. Lincoln Laboratory where substantial parts of the work were carried out, and the assistance of Gordon Holdsworth who performed the film evaporations.

Contents

	Page
	vii
List of Illustrations	
1 INTRODUCTION	1
2 METHOD OF DETECTION	2
3 THEORY OF GENERATION	3
4 EXPERIMENTAL RESULTS	12
5 CONCLUSIONS	18
References	21

Illustrations

Figure		Page
1	X-band phonon detection system	2
2	\vec{M} and \vec{H} vectors for arbitrary angles with film normal	4
3	Phonon paths from volume element in thin film to volume element in rod	6
4	Cross-sectional representation of uniform precession amplitude in thin film	7
5	Acoustic interference effects in thin film for spin-wave resonance and uniform precession cases	9
6	Superimposed phonon power peaks and SPWR absorption line	13
7	Phonon echoes at dc fields for peak in first echo for 83-17 permalloy, 4500 Å thick, on AC-cut quartz	13
8	Double phonon echo family for 90-10 permalloy, 4500 Å thick, on AC-cut quartz	14
9	Transverse mode generation with 90-10 permalloy, 4500 Å thick, on AC-cut quartz	15
10	Transverse and longitudinal modes in c-axis ruby at 77°K	16
11	Typical phonon echo saturation curve	17

Microwave Phonon Generation by Thin Magnetic Films*

1. INTRODUCTION

The two principle methods of generating phonons at microwave frequencies rely upon the piezoelectric and magnetostrictive effects. Piezoelectric generation in quartz has been extensively studied and is presently quite well understood.¹⁻³ Only recently has magnetostrictive generation been utilized in phonon interaction experiments.⁴ The method depends on the magnetostriction of a thin magnetic film which on resonance can emit phonons into an oriented rod. Bömmel and Dransfeld⁵ first demonstrated the feasibility of generating phonons in this way in a 1 kMcps experiment with a nickel film on quartz. Later Pomerantz⁶ generated phonons at 10 kMcps on SPWR in thin permalloy films. However, a detailed study of the actual generation process in the thin film has not yet been reported, although the probable generation model has been indicated by Bömmel and Dransfeld.⁵ Calculations and experimental data which provide further insight into the method of phonon generation in the thin film are presented, also included is factual information which should be of aid to those considering the use of thin films for phonon interaction studies or device applications.

* Presented at the 1962 Ultrasonics Symposium of the IRE Professional Group on Ultrasonics Engineering and to be published in the Transactions of the PGUE about March 1963.

2. METHOD OF DETECTION

The phonon detection system is shown in Figure 1. Pulsed microwave power from a 2J51 X-band magnetron is coupled into a rectangular TE 101 cavity. A thin magnetic film – single crystal rod system – is held in the cavity with a nylon screw and pressed against the cavity wall. On FMR or SPWR, phonons are generated in the film, enter the rod, are reflected from the far end of the rod, and return to re-excite FMR or SPWR in the film. The re-excited resonance creates a microwave pulse of the same width as the initial pulse in the cavity. This echo pulse radiates out of the cavity and is directed into the mixer by means of the circulator. There it is mixed with a STALO signal, amplified and displayed on the oscilloscope. An array of echoes is observed on the scope face since only a small portion of the phonon power in the rod is coupled out by the film on each reflection. The gradual decrease in echo amplitude is due to phonon attenuation in the rod and to other effects involving phonon propagation in the rod. In addition, a microwave calibration pulse of the same width as the magnetron pulse and of known power level is directed into the mixer. In this way, absolute echo heights can be measured. The minimum detectable echo power is approximately 10^{-14} watts or -110 dbm. When quartz is used as the single-crystal rod, this system and the rectangular cavity make possible the simultaneous observation of phonon echoes generated piezoelectrically and magnetostrictively.

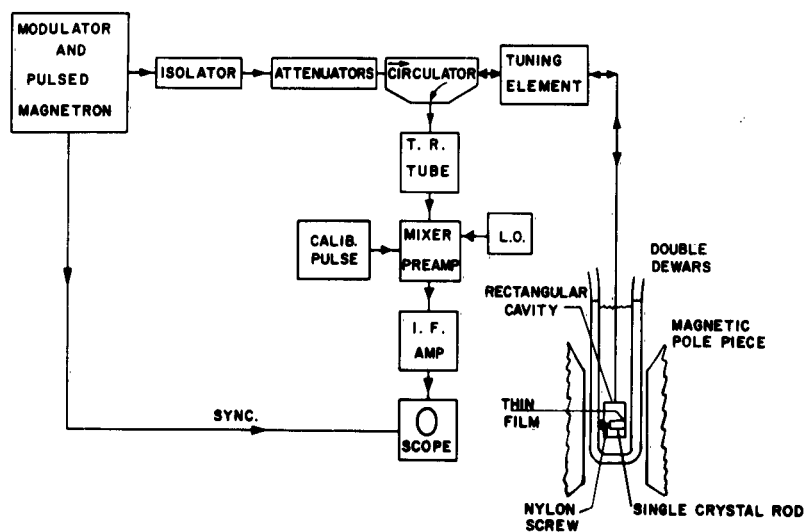


Figure 1. X-band Phonon Detection System

3. THEORY OF GENERATION

The generation of phonons by the film occurs because of magnetostriction. A stress ellipsoid precesses with the magnetization about the dc magnetic field.⁵ Variations with distance in the medium of the amplitude of this precessing stress provide sources of microwave phonons. The first step in the determination of the generated phonon power is to obtain the equations of motion for the displacement components. These contain driving terms proportional to the first derivative of the magnetostrictive stress and hence, to $b \, dm/dy$ where b is a magnetoelastic constant y the direction normal to the film, and m the microwave magnetization. The wave equations are solved by a Green's function method similar to that used by Jacobsen³ for the piezoelectric case. Then the phonon-power flow out of the film under acoustical match conditions can be noted immediately.

The equations of motion for small amplitudes are obtained from the following expression for the magnetoelastic energy density of a cubic crystal:⁷

$$U_c = \frac{b_1}{M^2} \left(M_x^2 e_{xx} + M_y^2 e_{yy} + M_z^2 e_{zz} \right) + \frac{b_2}{M^2} \left(M_x M_y e_{xy} + M_y M_z e_{yz} + M_z M_x e_{zx} \right) \quad (1)$$

where $\vec{M} = (M_x, M_y, M_z)$ is the magnetization, b_1 and b_2 are the magnetoelastic constants, and e_{ij} is a strain component. It is assumed that for the polycrystalline thin film, the axes of the demagnetizing ellipsoid coincide with the suitably averaged crystallographic axes. For highly oriented films or films having a preferred crystal-line axis oblique to the film plane, this coincidence of axes would not generally occur. Then the equations of motion given below would have different driving terms and the magnetoelastic constants would have somewhat different values. From Figure 2,

$$M_x = m_x \quad (2a)$$

$$M_y = M \cos \alpha + m_i \sin \alpha \quad (2b)$$

$$M_z = M \sin \alpha - m_i \cos \alpha \quad (2b)$$

where m_x and m_i are the microwave magnetizations and α is the angle between the film normal and the \vec{M} -direction. The following equations of motion for propagation

in the y-direction can be derived after Eqs. (2a, 2b, and 2c) are substituted into the energy expression in Eq. (1):

$$\frac{\partial^2 u}{\partial y^2} - \frac{1}{v_t^2} \frac{\partial^2 u}{\partial t^2} = -\frac{b_2}{c_{44}M} \cos \alpha \frac{\partial m_x}{\partial y} - \frac{b_2}{c_{44}M^2} \sin \alpha \frac{\partial(m_x m_i)}{\partial y} \quad (3a)$$

$$\frac{\partial^2 v}{\partial y^2} - \frac{1}{v_i^2} \frac{\partial^2 v}{\partial t^2} = -\frac{b_1}{(c_{12}+2c_{44})M} \sin 2\alpha \frac{\partial m_i}{\partial y} - \frac{b_1}{(c_{12}+2c_{44})M^2} \sin \alpha \frac{\partial m_i^2}{\partial y} \quad (3b)$$

$$\frac{\partial^2 w}{\partial y^2} - \frac{1}{v_t^2} \frac{\partial^2 w}{\partial t^2} = \frac{b_2}{c_{44}M} \cos 2\alpha \frac{\partial m_i}{\partial y} + \frac{b_2}{2c_{44}M^2} \sin 2\alpha \frac{\partial m_i^2}{\partial y} \quad (3c)$$

where the displacement $\vec{\rho} = (u, v, w)$ and where b_1 and b_2 are now suitably averaged magnetoelastic constants.

The first term on the right of each equation is a magnetostrictive-phonon driving term at the precession frequency. In general, these terms are present for both transverse modes [Eqs. (3a and 3c)] and the longitudinal mode [Eq. (3b)]. For $\alpha = 0^\circ$ and 90° ; however, only transverse modes can be generated. It is evident from Eq. (3b) that the longitudinal mode-driving term is a maximum at $\alpha = 45^\circ$ for constant dm_i/dy and goes to 0 at $\alpha = 0^\circ$ and 90° .

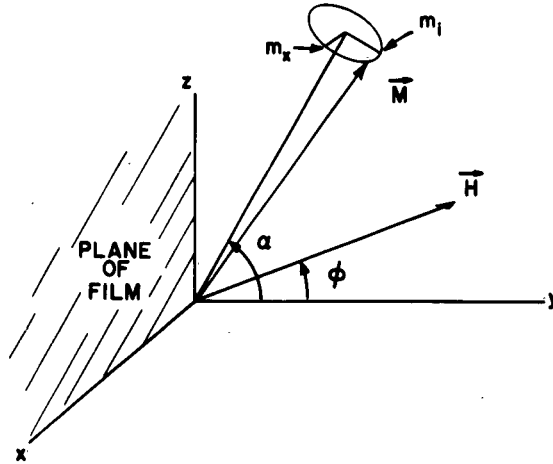


Figure 2. \vec{M} and \vec{H} vectors for Arbitrary Angles With Film Normal. The axis of the substrate rod lies along the y-direction and also the phonon propagation direction.

Because of their quadratic m -dependence the second terms on the right of each equation are driving terms for phonons of frequency 2ω . The existence of such terms was indicated earlier by Bömmel and Dransfeld.⁵ The 2ω terms are smaller than the ω terms by a factor of the order of the precession angle, m/M .

In the area of spin wave-phonon crossover (equal k and ω) the full set of coupled magnetoelastic equations must be solved in order to find the displacement components. However, except for a small magnetic field region of the SPWR spectrum, crossover does not appear to be important for this type of thin magnetic film-phonon generation. This is evident in the case of the uniform precession where the $k \cong 0$ spin wave is excited. In a SPWR experiment, the field at crossover is

$$H_{cr} = \frac{\omega}{\gamma} - \frac{2A}{M} k_p^2 \quad (4)$$

At X-band, for $A \sim 10^{-6}$ ergs/cm, $4\pi M = 10^4$ oe and $k_p = 2 \times 10^5$ cm⁻¹, $(\omega/\gamma - H_{cr}) \sim 100$ oe. For most of the SPWR fields, $(\omega/\gamma - H_{cr}) > 100$ oe. Also, the width of the region where any appreciable splitting occurs has been shown by the author⁸ to be less than approximately 80 oe for a 60 oe SPWR-line width and for $b_2 = 4 \times 10^7$ ergs/cm³. Pomerantz⁹ has suggested that due to spin-wave damping in a SPWR experiment, discrete k -values are not excited and a series expansion of the damped spin wave would include k -values in the crossover region. Although this may be a consideration, it is not treated here.

The solutions of the inhomogeneous wave Eqs. (3a, 3b, and 3c) can now be obtained by a Green's function method similar to that used by Jacobsen³ in the case of piezoelectric generation. When an acoustical match between the film and substrate rod is assumed, the solution for the u -component of the displacement neglecting the 2ω driving terms is

$$u = \int_0^{\infty} G(y, y') \left[-\frac{b_2}{c_{44}M} \cos \alpha \frac{dm_x}{dy'} \right] dy' \quad (5)$$

Similar relations can be noted for the v - and w -components. The Green's function, $G(y, y')$, appearing in Eq. (5) is the sum function for the direct wave and the wave reflected from $y'=0$ (see Figure 3). Thus since

$$G(y) = \frac{i}{2k_p} e^{-ik_p y} \quad (6)$$

we obtain

$$G(y, y') = G(y-y') + G(y+y') = \frac{i}{k} \cos k_p y' e^{-ik_p y} \quad (7)$$

Hence,

$$u = -\frac{ib_2 \cos \alpha}{k_p c_{44} M} \left[\int_0^d \frac{dm}{dy} \cos k_p y dy \right] e^{-ik_p y} \quad (8)$$

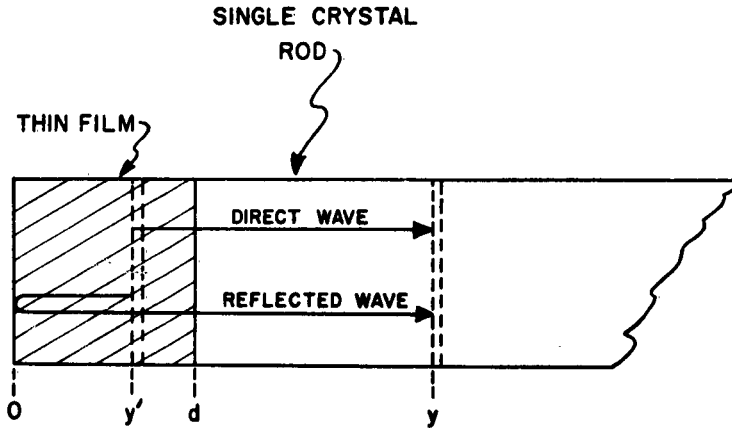


Figure 3. Phonon Paths From Volume Element in Thin Film to Volume Element in Rod. The net phonon amplitude at y is the sum of the amplitudes for the direct and reflected waves.

Therefore, the phonon generation is determined by the integral across the film thickness of the microwave magnetic-field gradient weighted by the $\cos k_p y$ factor from the Green's function. In the uniform precession case this integral receives contributions only from the film surfaces since dm/dy is 0 throughout the film interior. From Figure 4 it is seen that in the limiting case when the trapezoid becomes a rectangle,

$$\frac{dm}{dy} = m_0 [\delta(y) - \delta(y-d)] \quad (9)$$

A delta-function driving term exists at each film surface. Thus the u -component in

the uniform precession case becomes

$$u = - \frac{ib_2 \cos \alpha}{k_p c_{44} M} (1 - \cos k_p d) m_x^o \quad (10)$$

When the dc magnetic field is parallel to the film plane ($\alpha = 90^\circ$),

$$u = v = 0 \quad (11a)$$

$$w = \frac{-ib_2}{k_p c_{44} M} (1 - \cos k_p d) m_y^o \quad (11b)$$

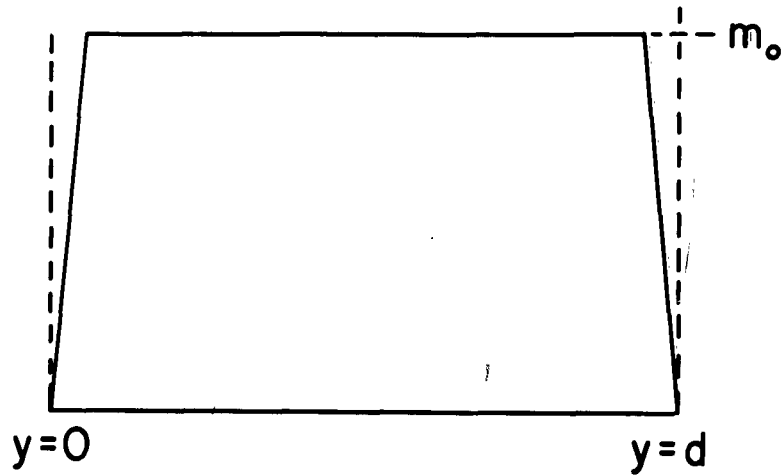


Figure 4. Cross-Sectional Representation of Uniform Precession Amplitude in Thin Film. The slopes at $y=0$ and $y=d$ are $+\infty$ and $-\infty$ respectively in the actual case. The slope of m is given by Eq. (9).

A transverse phonon polarized parallel to the dc magnetic field direction and proportional to the normal component of the microwave magnetization is generated. In the case of a perfect acoustical match, the phonon power flow per unit area out of the film and into the substrate rod is,

$$\begin{aligned} P_{ac} &= U_e v_t \\ &= \frac{1}{2} c_{44} \left| \frac{dw}{dy} \right|^2 v_t \end{aligned}$$

$$= \frac{b_2^2 v_t}{2 c_{44}} \left(\frac{m_y^o}{M} \right)^2 \left(1 - \cos k_p d \right)^2 \quad (12)$$

When the dc magnetic field is perpendicular to the film plane ($\alpha=0^\circ$), a similar calculation yields:

$$P_{ac} = \frac{b_2^2 v_t}{2 c_{44}} \left(\frac{m_o}{M} \right)^2 (1 - \cos k_p d)^2 \quad (13)$$

Here m_o is the amplitude of the circular rotating microwave magnetization. A circular polarized phonon is generated. A formula similar to Eq. (13), except for the $(1 - \cos k_p d)^2$ factor, has been given by Bömmel and Dransfeld.⁵

The expression for the phonon-power flow for the case of SPWR (also the $\alpha=0^\circ$ case) is

$$P_{ac} = \frac{b_2^2 v_t}{2 c_{44}} \left(\frac{|I|}{M} \right)^2 \quad (14)$$

where

$$I = \int_0^d \frac{dm}{dy} \cos k_p y dy \quad (15)$$

If the spins are pinned at the film surfaces, no delta-function terms appear in the dm/dy expression. The generation takes place throughout the interior of the film.

Calculations of P_{ac} versus dc magnetic field have been made based on a previous publication by the author.¹⁰ The results show that the phonon-power peak associated with a SPWR line can be shifted off the line by as much as 40 oe for a 50 oe SPWR line width at X-band. This shift is caused by the interference between acoustic waves originating in different parts of the film. In the uniform precession case, the interference is expressed mathematically by the $(1 - \cos k_p d)^2$ factor in Eqs. (12) and (13). Figure 5 illustrates this interference for the case of a film just 3/4 of a phonon wavelength thick ($\sim 3330\text{\AA}$ at X-band). The Green's function weighting factor is the $\cos \frac{3\pi}{2} \frac{y}{d}$ curve and the dm/dy term is given by $\sin k(y - \frac{d}{2})$ where $k = \sqrt{\frac{M}{2A}} (\omega/\gamma - H)$. In the SPWR case the regions of + and - contribution to the net phonon power are respectively unshaded and shaded in the figure. In the direction of decreasing H, the + regions grow at the expense of the - regions. The net phonon power would then

decrease in this direction if the SPWR peak were not present at $H = H_3$. Since the SPWR peak contributes a resonance denominator to the phonon power-flow expression, the phonon power peak is shifted to a field larger than H_3 .

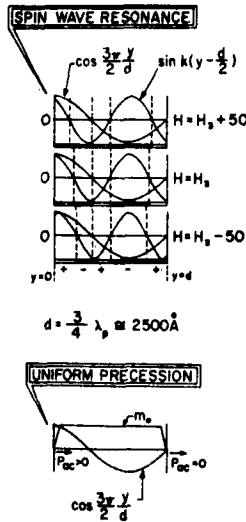


Figure 5. Acoustic Interference Effects in Thin Film For Spin-wave Resonance and Uniform Precession Cases. The Green's function and m -amplitude are shown in the film cross sections. Phonon power flow is in the $+y$ -direction.

In the uniform precession case in Figure 5 all the phonon power is seen to emerge from the $y = 0$ surface. Destructive interference occurs for waves originating at the $y = d$ surface; the wave reflected from $y = 0$ must travel $\frac{3}{2} \lambda_p$ further than the direct wave from $y = d$. For films an odd number of $\frac{1}{2} \lambda_p$ phonon wavelengths thick, the maximum phonon power is generated. However, for an even number of $\frac{1}{2} \lambda_p$ phonon wavelengths, destructive interference completely cancels the phonon generation.

For a comparison of theory with experiment an expression must be obtained for the ratio of echo power out of the rectangular cavity to input power. Since $Q_u = \omega h^2 V_{cav} / 8\pi P_{in}$ and $|m| = |\chi| h$ where χ is the susceptibility, we have for the uniform precession case, using Eq. (12) or (13),

$$\frac{P_{ac}}{P_{in}} = \frac{4\pi b_2^2 |\chi|^2 (1 - \cos k_d d)^2}{c_{44} M^2} \frac{A_f v Q_u}{\omega V_{cav}} \quad (16)$$

This assumes that the film is situated in the maximum h-field region. If the substrate rod is also within the cavity volume, the fields are greatly perturbed; but Eq. (16) may still be used for order of magnitude estimates. In the case of SPWR, $|\chi| (1 - \cos k_p d)$ is replaced by $|I|/h$.

The output-input power ratio below the nonlinear resonance region for the film may be found by squaring Eq. (16). This assumes that the conversion efficiency from acoustic to magnetic energy is the same as that from magnetic to acoustic and that there is negligible loss to the substrate rod in the first round trip of the phonon echo. At critical coupling to the cavity, the power ratio is thus:

$$\frac{P_o}{P_{in}} = K_{mm}^4 \left(\frac{A_f v Q_u}{\omega V_{cav}} \right)^2 \quad (17)$$

where K_{mm} is the magneto-mechanical coupling coefficient and is given by:

$$K_{mm}^2 = \frac{4\pi b_2^2 |\chi|^2 (1 - \cos k_p d)^2}{c_{44} M^2} \quad (18)$$

Thus the output-input power ratio for a given film is a constant independent of input power up to the instability threshold. Above the threshold, the susceptibility begins to decrease. The power ratio decreases only as the square of the susceptibility, however, and not as the fourth power. This is caused by the return echo pulse arriving at the film when the exciting pulse is off. Since the echo power is much smaller than the driving power, FMR or SPWR is re-excited in the low power region where χ is a constant. Thus for incident powers in the high power region,

$$\frac{P_o}{P_{in}} = \left(\frac{4\pi b_2^2}{c_{44} M^2} \right)^2 \chi^2 \chi_o^2 \left(\frac{A_f v Q_u}{\omega V_{cav}} \right)^2 \quad (19)$$

where χ_o is the low power susceptibility and χ is the high power susceptibility. Since $\chi = m_o/h$ where m_o is a constant at high powers and since $P_{in} \sim h^2$, P_o is a constant above the instability threshold. Therefore, the echo amplitudes saturate at high power levels and the output-input power ratio decreases.

It is now possible to make a theoretical comparison of the phonon generation efficiencies in the magnetostrictive and piezoelectric cases. In the latter case,

This assumes that the film is situated in the maximum h-field region. If the substrate rod is also within the cavity volume, the fields are greatly perturbed; but Eq. (16) may still be used for order of magnitude estimates. In the case of SPWR, $|\chi| (1 - \cos k_p d)$ is replaced by $|I|/h$.

The output-input power ratio below the nonlinear resonance region for the film may be found by squaring Eq. (16). This assumes that the conversion efficiency from acoustic to magnetic energy is the same as that from magnetic to acoustic and that there is negligible loss to the substrate rod in the first round trip of the phonon echo. At critical coupling to the cavity, the power ratio is thus:

$$\frac{P_o}{P_{in}} = K_{mm}^4 \left(\frac{A_f v Q_u}{\omega V_{cav}} \right)^2 \quad (17)$$

where K_{mm} is the magneto-mechanical coupling coefficient and is given by:

$$K_{mm}^2 = \frac{4\pi b_2^2 |\chi|^2 (1 - \cos k_p d)^2}{c_{44} M^2} \quad (18)$$

Thus the output-input power ratio for a given film is a constant independent of input power up to the instability threshold. Above the threshold, the susceptibility begins to decrease. The power ratio decreases only as the square of the susceptibility, however, and not as the fourth power. This is caused by the return echo pulse arriving at the film when the exciting pulse is off. Since the echo power is much smaller than the driving power, FMR or SPWR is re-excited in the low power region where χ is a constant. Thus for incident powers in the high power region,

$$\frac{P_o}{P_{in}} = \left(\frac{4\pi b_2^2}{c_{44} M^2} \right)^2 \chi^2 \chi_o^2 \left(\frac{A_f v Q_u}{\omega V_{cav}} \right)^2 \quad (19)$$

where χ_o is the low power susceptibility and χ is the high power susceptibility. Since $\chi = m_o/h$ where m_o is a constant at high powers and since $P_{in} \sim h^2$, P_o is a constant above the instability threshold. Therefore, the echo amplitudes saturate at high power levels and the output-input power ratio decreases.

It is now possible to make a theoretical comparison of the phonon generation efficiencies in the magnetostrictive and piezoelectric cases. In the latter case,

$$\frac{P_{ac}}{P_{in}} = K_{em}^2 \left(\frac{AvQ_u}{\omega V_{cav}} \right) \quad (20)$$

where for quartz

$$K_{em}^2 = \frac{4\pi e_{11}^2}{c_{11}\epsilon} \sim 10^{-2} \quad (21)$$

In the thin film magnetostrictive case and for the uniform precession on resonance

$$K_{mm}^2 = \frac{4\pi b_2^2 (1 - \cos k_p d)^2}{c_{44} (\Delta H)^2} \quad (22)$$

For a 90-10 permalloy film an odd number of half-wavelengths thick and having $\Delta H \sim 120$ oe and $b_2 = -4 \times 10^7$ ergs/cm³,

$$K_{mm}^2 \sim 3$$

The elastic constant c_{44} is taken as 10^{12} dynes/cm² which is approximately true for both ruby and quartz. The magnetostrictive generation in this case appears to be two orders of magnitude more efficient than the piezoelectric for the same $(AvQ/\omega V)$ factor. This factor, however, is larger for a quartz rod in a re-entrant cavity than it is for a film-rod system in a rectangular cavity. In the former case, a typical value for Aq/V_{cav} is 10 cm⁻¹ and for $Q_u = 1000$, $v = 3 \times 10^5$ cm/sec, $\omega = 6.28 \times 10^{10}$, we have $(AvQ/\omega V) \cong 5 \times 10^{-2}$. For a .25-inch diameter film in a TE 101 rectangular cavity, $A_f/V_{cav} \cong .05$ cm⁻¹ and for $Q_u = 1500$, $v = 3 \times 10^5$ cm/sec, $\omega = 6.28 \times 10^{10}$, we have $(AvQ/\omega V) \cong 3.6 \times 10^{-4}$. Table 1 gives a comparison of the two cases at 9000 Mcps assuming that the thin film is acoustically matched to the substrate.

TABLE 1

Process	Material	Cavity	K^2	P_{ac}/P_{in}	P_o/P_{in}
Piezoelectric	Quartz	Re-entrant	10^{-2}	$.5 \times 10^{-3}$	$.25 \times 10^{-6}$
Magnetostrictive	90-10 permalloy $\Delta H = 120$ oe	TE 101	3	10^{-3}	10^{-6}

The output-input power ratios are about the same order of magnitude. Filling factor improvements can be made in the magnetostrictive case, however, by enhancing the microwave magnetic field through improved cavity design.¹¹ Also, the coupling coefficient can be improved by increasing the $b_2/\Delta H$ ratio.

4. EXPERIMENTAL RESULTS

Phonon echoes have been observed in the X-band frequency region using permalloy films of various compositions and thicknesses. The optically polished and oriented rods used have consisted of either AC- or X-cut quartz or c-axis ruby. The films are evaporated onto one end face of a rod. The echoes are observed at various film normal-dc magnetic field angles between 0° and 90° . Nearly all of the experiments have been conducted at 4°K , but in the case of ruby a few have been conducted at 77°K . The phonon echo power radiated out of the cavity has been measured and echo saturation effects have been observed at the higher input power levels.

A. Perpendicular Case ($\alpha=0^\circ$)

Separate echo maxima at different dc magnetic fields for a fixed film orientation have been observed only when the film normal is parallel, or nearly parallel, to the dc magnetic field. Each echo peak can usually be identified with a certain SPWR absorption line. However, the peaks do not generally coincide in dc-field with the lines and in some cases, the identification cannot be made on a one-to-one basis. Figure 6 illustrates the latter situation for an 88-12 permalloy film, 4500 \AA thick, on a c-axis ruby rod at 77°K . There are six echo peaks and only five SPWR lines (including a 'kink' on the high field side of the main resonance). Another interesting feature of the curve is that the echo power falls to 0 between the peaks, whereas the resonance absorption maintains itself at a relatively high level. At 77°K no more than two transverse echoes are ever observed. The attenuation in the ruby is greater than 10 db/cm . At 4°K , however, many transverse echoes are observed and the attenuation is less than $.2 \text{ db/cm}$. Now at 4°K the odd-numbered return echoes all peak at approximately the same dc-fields. These fields are essentially the same as shown in Figure 6 for the single (first) echo at 77°K . The even-numbered return echoes, however, have their maxima at field values somewhere between those shown in Figure 6. An alternation in height of successive echoes occurs and is a function of dc magnetic field. If a highly warped phonon-wave shape over the rod cross section were generated on SPWR so that large phase variations over the rod-end faces occurred, the effect could be qualitatively explained. The effect occurs with AC- and X-cut quartz substrates as well as with ruby and is observed only under SPWR conditions. Also it is independent of small angles between the film normal and dc magnetic field, provided SPWR is observed.

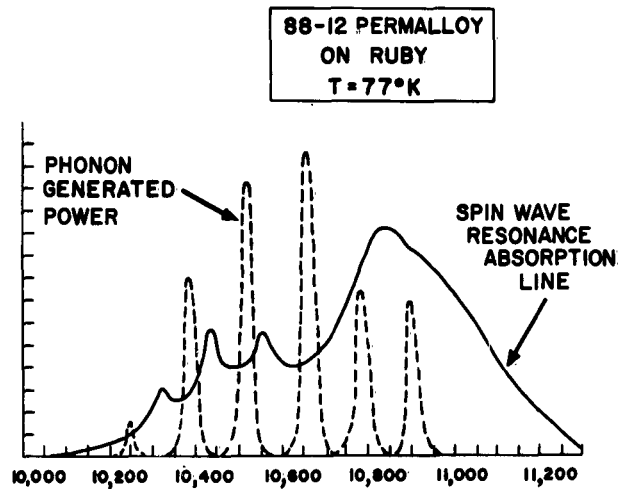


Figure 6. Superimposed Phonon Power Peaks and SPWR Absorption Line. The film thickness is $\sim 4500\text{\AA}$ and the phonon power is that in the first return transverse mode echo.

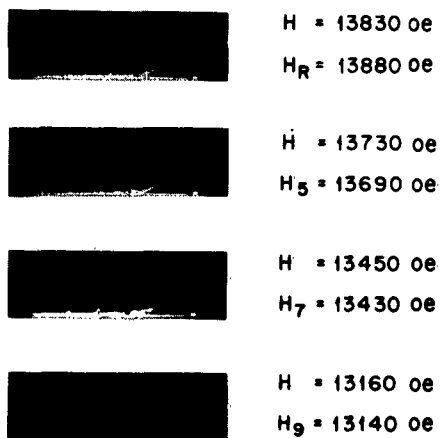
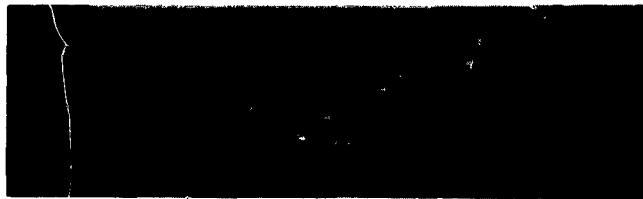


Figure 7. Phonon Echoes at dc Fields for Peak in First Echo for 83-17 Permalloy, 4500 \AA Thick, on AC-cut Quartz. The resonance peak fields are given below the echo peak fields beside each film strip.

The more typical case in which each phonon echo peak can be identified with a SPWR line is shown in Figure 7. The phonon echo peak fields apply to the first return echo, but in this case, the second echo fields are very near the first echo fields. The shifts of from 20 oe to 50 oe shown in the figure could be explained by the interference effect previously described. For the 83-17 permalloy composition the magnetoelastic constant, b , should be close to 0. The observability of phonon echoes for this composition suggests that phonon echo studies may provide a sensitive means for exploring the zero magnetostriction region for permalloy.

The maximum phonon echo power appears to be associated with the $p = 7$ line in Figure 7. This line is over 400 oe below the main line and hence, cannot be associated with the crossover region which is ~ 100 oe below the main line. It is characteristic that in the SPWR generation of phonons, the maximum echo power appears between 300 oe and 500 oe below the main line. Also, each SPWR line usually has a phonon peak associated with it and no particularly unique results occur in the region where crossover is expected. The theoretical computations mentioned in the previous section are based on Eqs. (14) and (15) which do not take crossover into account. The results give phonon peak values which appear to be of the correct order of magnitude in the area of the main resonance, but fall off too rapidly with decreasing dc magnetic field. Not accounted for are the large echo powers observed for peaks more than ~ 300 oe below the main resonance.



$$H = H_R$$

Figure 8. Double Phonon Echo Family for 90-10 Permalloy, 4500Å Thick, on AC-cut Quartz. Only 15 mw peak power is incident on the cavity and the output-input power ratio is $\sim 10^{-7}$.

Figure 8 shows the simultaneous generation of the two transverse modes in AC-cut quartz. This double echo family is expected since a circular polarized phonon is generated in the perpendicular case ($\alpha = 0^\circ$). This figure also illustrates one of the rare instances in which there is an echo peak (in this case for both even- and odd-return echoes) within 10 oe of the main resonance absorption.

The peak power incident on the cavity for the echoes shown in Figure 8 is only 15 mw and the output-input power ratio is $\sim 10^{-7}$. This is an order of magnitude less than the 10^{-6} value given in Table 1 for a film of the same composition. The discrepancy is partly due to the deviation of the actual film thickness from $\frac{3}{2} \lambda_p \approx 5000\text{\AA}$. Also, since the power ratio varies as b^4 , a decrease in b-value by a factor of $10^{1/4} = 1.78$ would explain the discrepancy. The effect of film-substrate acoustical mismatch, although difficult to determine, is believed to be small since otherwise large echo attenuation would be observed.

B. Parallel Case ($\alpha = 90^\circ$)

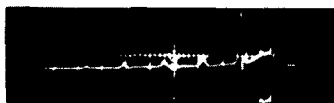
The output-input power ratio in the parallel case is from 10^{-2} to 10^{-3} times smaller than it is in the perpendicular case. This appears to be caused in part by the smaller microwave m-value in the parallel case for the same susceptibility and microwave h-value. At X-band and for $4\pi M = 7000$ oe, $m_y^0/m_o \approx (\omega/\gamma)/(H_r + 4\pi M) \approx .38$ and hence $(m_y^0/m_o)^4 = 2 \times 10^{-2}$. When other factors are equal $(m_y^0/m_o)^4$ is just the relative power ratio of the two cases. Thus the observed relative power ratio is nearly accounted for by the $(m_y^0/m_o)^4$ ratio.



EASY DIRECTION

$$H = H_R = 800 \text{ oe}$$

$$v_{t1} = 3.30 \cdot 10^5 \text{ cm/sec}$$



HARD DIRECTION

$$H = H_R = 1210 \text{ oe}$$

$$v_{t2} = 3.80 \cdot 10^5 \text{ cm/sec}$$

Figure 9. Transverse Mode Generation With 90-10 Permalloy, 4500 \AA thick, on AC-cut Quartz.

Since the generated phonon is linearly polarized along the dc magnetic field direction, the two orthogonal transverse modes in AC-cut or X-cut quartz can be separately excited. Figure 9 shows separate echo families in AC-cut quartz for the dc-field along the easy and hard directions of magnetic anisotropy. The film anisotropy axis is apparently related to the quartz crystallographic axes since only the 3.3×10^5 cm/sec transverse mode is generated in the easy direction and only the 3.80×10^5 cm/sec transverse mode is generated in the hard direction. The magnitude of the anisotropy is much larger than is usual for permalloy films of this composition.

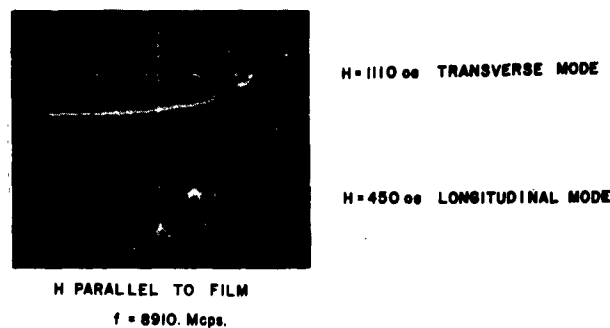


Figure 10. Transverse and Longitudinal Modes in c-axis Ruby at 77°K. At 4°K the attenuations of the transverse and longitudinal modes are nearly the same.

Only transverse mode echoes are observed on resonance in the parallel case. However, off resonance longitudinal mode echoes have been observed. Figure 10 shows such echoes as well as the transverse mode echo on resonance at 77°K for a 90-10, 4500 Å film on ruby. These longitudinal echoes may be generated from the subsidiary absorption peak which can occur at high power levels in a FMR experiment. Also it may be noticed that the attenuation of the longitudinal modes echoes is much less than that for the transverse. At 4°K the attenuations are approximately equal. Thus the attenuation of transverse waves in c-axis ruby increases with temperature much faster than that for the longitudinal waves.

C. Intermediate Angles

Longitudinal mode echoes on resonance are observed only at α -angles between 0° and 90°. The echoes are largest for angles between 20° and 45°. If the microwave m-value for a given susceptibility and microwave h-value did not vary with angle, the theoretical maximum for longitudinal mode generation would occur at $\alpha = 45^\circ$. However, the m-value increases as the dc magnetic field for resonance approaches the perpendicular orientation ($\alpha = 0^\circ$). Thus the theoretical maximum must

occur between 45° and 0°; this is in qualitative agreement with experiment.

TABLE 2. Output-input power ratios for different angles between \vec{M} and film normal

α	H_R	Transverse Echoes	Longitudinal Echoes
90°	1040 oe	$.002 \times 10^{-10}$	-
70°	3140	-	$.05 \times 10^{-10}$
45°	6040	-	$.71 \times 10^{-10}$
20°	8990	-	$.81 \times 10^{-10}$
0°	10000	$.5 \times 10^{-10}$	-

Table 2 lists output-input power ratios at different α -values for a 90-10 permalloy film, 3000 Å thick, on ruby at 4°K. The α -values were obtained from theoretical curves prepared by P. E. Wigen¹² permitting α , the resonance field, and the angle between H and the film normal to be simultaneously obtained. The low output-input power ratio value of 0.5×10^{-10} for the $\alpha=0^\circ$ case can be partly explained by the closeness of the film thickness to $\lambda p \approx 3330$ Å. However, not understood is the fact that the phonon peak falls on the tail of the main peak about 200 oe above the resonance field.

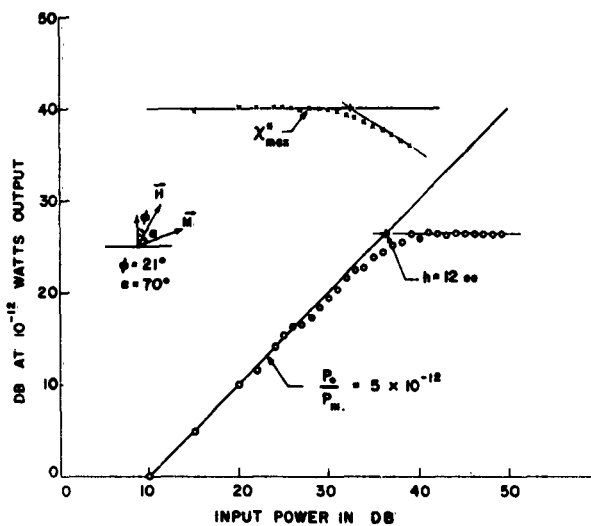


Figure 11. Typical Phonon Echo Saturation Curve. The decay of the susceptibility is also shown.

D. High Powers

A typical phonon echo saturation curve is shown in Figure 11. The film-substrate system used is the same as for Table 2 and the data were taken for $\alpha=70^\circ$. The attenuation in db needed to keep the power in the first return echo at a 10^{-12} watt level is plotted versus the input power entering the cavity. For input powers up to 33 db a straight-line relation is obtained. This implies a constant P_o/P_{in} value, in this case 5×10^{-12} , in accordance with theory. Above 38 db input the echo height is constant independent of input power as theoretically predicted for powers above the instability threshold. The imaginary part of the susceptibility versus input power is also shown. The threshold field determined from the echo measurements is in close agreement with that from the susceptibility measurements. For a second order nonlinearity, and for $\Delta H = \Delta H_k = 130$ oe and $4\pi M = 7000$ oe, $h_{cr} = 18$ oe is in reasonable agreement with the $h=12$ oe experimental value.

Phonon echo saturation has been observed at other angles between H and the film normal and also on SPWR. Echo saturation experiments should provide a new and sensitive means for studying high power effects on FMR or SPWR in thin magnetic films.

5. CONCLUSIONS

Certain qualitative results of the generation theory presented in Section 3 are exhibited in the experimental data. These results hold mainly in the uniform precession FMR case and are as follows:

- (1) Simultaneous generation of two transverse modes in the perpendicular case ($\alpha=0^\circ$)
- (2) Separate generation of transverse modes in the parallel case ($\alpha=90^\circ$)
- (3) Absence of longitudinal mode for $\alpha=0^\circ$ and $\alpha=90^\circ$
- (4) Maximum in longitudinal mode for $20^\circ < \alpha < 45^\circ$
- (5) Constant value of P_o/P_{in} up to the instability threshold
- (6) Constant value of P_o above the threshold.

In addition, the quantitative prediction of P_o/P_{in} has been checked except for an order of magnitude discrepancy which can be reasonably accounted for. The ratio of echo powers in the parallel and perpendicular cases has also received approximate quantitative verification.

The qualitative and partial quantitative agreement of theory and experiment lends support to the generation model discussed in Section 3. However, in the case of SPWR generation there are several experimental features which remain largely unexplained. These are as follows:

- (1) Large 'beating' effect in the phonon echo envelope in certain cases. The effect varies markedly with dc magnetic field.

- (2) Much larger echo powers than expected for high SPWR p-numbers.
- (3) Apparent absence of crossover phenomena.
- (4) Shift of phonon peak off SPWR peak (partially explained by interference effect).
- (5) Presence of extra peaks not associated with any particular SPWR line in certain cases.

Other mechanisms not considered in this report may be active in the phonon generation in the SPWR case.

Additional studies suggested by this work are: (1) investigation of zero magnetostriction region in permalloy, (2) high power resonance investigations in thin films by observing echo saturation.

Finally, the electromagnetic to acoustic conversion efficiencies for quartz and 90-10 permalloy have been shown to be approximately the same. However, in the case of magnetostrictive generation, substantial improvement seems possible.

References

1. E. G. Cook and H. E. Van Valkenburg, *J. Acoust. Soc. Am.* 27, 564 (1955).
2. H. E. Bömmel and K. Dransfeld, *Phys. Rev.* 117, 1245 (1960).
3. E. H. Jacobsen, *J. Acoust. Soc. Am.* 32, 949 (1960).
4. M. Pomerantz, R. W. Keyes, and P. E. Seiden, *Phys. Rev. Letters* 9, 312 (1962).
5. H. E. Bömmel and K. Dransfeld, *Phys. Rev. Letters* 3, 83 (1959).
6. M. Pomerantz, *Phys. Rev. Letters* 7, 312 (1961).
7. C. Kittel, *Rev. Mod. Physics* 21, 541 (1949).
8. M. H. Seavey, Jr., Lincoln Lab. Group Rpt. 82G-0029, 31 July 1961.
9. M. Pomerantz, *Bull. Am. Phys. Soc.* 7, 189 (1962).
10. M. H. Seavey, Jr., Lincoln Laboratory Technical Report No. 239, 15 Feb 1961.
11. H. Hsu, W. Brouillette, and S. Wanuga, 1962 Ultrasonics Symposium of IRE PGUE (to be published).
12. P. E. Wigen, private communication.

<p>Air Force Cambridge Research Laboratories Geophysics Research Directorate L. G. Hanscom Field, Bedford, Mass.</p> <p>MICROWAVE PHONON GENERATION BY THIN MAGNETIC FILMS*, by M. H. Seavey, Jr., February 1963. 21 p. AFCL-63-57. Unclassified report.</p> <p>The magnetostrictive generation of microwave phonons by thin magnetic films is theoretically described and experimental data taken at X-band are discussed. The cases of generation on the uniform precession on ferromagnetic resonance (FMR) and on spin-wave resonance (SPWR) are treated. Wave equations are obtained for the displacement components when the dc magnetic field makes an arbitrary angle with the film normal. These have driving terms proportional to dm/dy which are responsible for the phonon generation. It is shown that in the FMR case the generation occurs at the film surfaces while in the SPWR case the generation takes place throughout the film interior. The experimental data appear to support the generation model in the FMR case, but unexplained discrepancies exist between</p> <p style="text-align: right;">(over)</p>	<p>Air Force Cambridge Research Laboratories Geophysics Research Directorate L. G. Hanscom Field, Bedford, Mass.</p> <p>MICROWAVE PHONON GENERATION BY THIN MAGNETIC FILMS*, by M. H. Seavey, Jr., February 1963. 21 p. AFCL-63-57. Unclassified report.</p> <p>The magnetostrictive generation of microwave phonons by thin magnetic films is theoretically described and experimental data taken at X-band are discussed. The cases of generation on the uniform precession on ferromagnetic resonance (FMR) and on spin-wave resonance (SPWR) are treated. Wave equations are obtained for the displacement components when the dc magnetic field makes an arbitrary angle with the film normal. These have driving terms proportional to dm/dy which are responsible for the phonon generation. It is shown that in the FMR case the generation occurs at the film surfaces while in the SPWR case the generation takes place throughout the film interior. The experimental data appear to support the generation model in the FMR case, but unexplained discrepancies exist between</p> <p style="text-align: right;">(over)</p>	<p>UNCLASSIFIED</p> <ol style="list-style-type: none"> 1. Thin Films 2. Magnetostriction Transducers 3. Phonons <p>I. Seavey, M. H., Jr.</p> <p>UNCLASSIFIED</p>	<p>UNCLASSIFIED</p> <ol style="list-style-type: none"> 1. Thin Films 2. Magnetostriction Transducers 3. Phonons <p>I. Seavey, M. H., Jr.</p> <p>UNCLASSIFIED</p>
<p>Air Force Cambridge Research Laboratories Geophysics Research Directorate L. G. Hanscom Field, Bedford, Mass.</p> <p>MICROWAVE PHONON GENERATION BY THIN MAGNETIC FILMS*, by M. H. Seavey, Jr., February 1963. 21 p. AFCL-63-57. Unclassified report.</p> <p>The magnetostrictive generation of microwave phonons by thin magnetic films is theoretically described and experimental data taken at X-band are discussed. The cases of generation on the uniform precession on ferromagnetic resonance (FMR) and on spin-wave resonance (SPWR) are treated. Wave equations are obtained for the displacement components when the dc magnetic field makes an arbitrary angle with the film normal. These have driving terms proportional to dm/dy which are responsible for the phonon generation. It is shown that in the FMR case the generation occurs at the film surfaces while in the SPWR case the generation takes place throughout the film interior. The experimental data appear to support the generation model in the FMR case, but unexplained discrepancies exist between</p> <p style="text-align: right;">(over)</p>	<p>Air Force Cambridge Research Laboratories Geophysics Research Directorate L. G. Hanscom Field, Bedford, Mass.</p> <p>MICROWAVE PHONON GENERATION BY THIN MAGNETIC FILMS*, by M. H. Seavey, Jr., February 1963. 21 p. AFCL-63-57. Unclassified report.</p> <p>The magnetostrictive generation of microwave phonons by thin magnetic films is theoretically described and experimental data taken at X-band are discussed. The cases of generation on the uniform precession on ferromagnetic resonance (FMR) and on spin-wave resonance (SPWR) are treated. Wave equations are obtained for the displacement components when the dc magnetic field makes an arbitrary angle with the film normal. These have driving terms proportional to dm/dy which are responsible for the phonon generation. It is shown that in the FMR case the generation occurs at the film surfaces while in the SPWR case the generation takes place throughout the film interior. The experimental data appear to support the generation model in the FMR case, but unexplained discrepancies exist between</p> <p style="text-align: right;">(over)</p>	<p>UNCLASSIFIED</p> <ol style="list-style-type: none"> 1. Thin Films 2. Magnetostriction Transducers 3. Phonons <p>I. Seavey, M. H., Jr.</p> <p>UNCLASSIFIED</p>	<p>UNCLASSIFIED</p> <ol style="list-style-type: none"> 1. Thin Films 2. Magnetostriction Transducers 3. Phonons <p>I. Seavey, M. H., Jr.</p> <p>UNCLASSIFIED</p>

<p>theory and experiment in the SPWR case. A comparison with quartz piezoelectric generation is made and while the generation efficiencies are about equal, substantial improvement is possible in the magnetostrictive case.</p>	<p>theory and experiment in the SPWR case. A comparison with quartz piezoelectric generation is made and while the generation efficiencies are about equal, substantial improvement is possible in the magnetostrictive case.</p>	<p>UNCLASSIFIED</p>	<p>UNCLASSIFIED</p>
<p>theory and experiment in the SPWR case. A comparison with quartz piezoelectric generation is made and while the generation efficiencies are about equal, substantial improvement is possible in the magnetostrictive case.</p>	<p>theory and experiment in the SPWR case. A comparison with quartz piezoelectric generation is made and while the generation efficiencies are about equal, substantial improvement is possible in the magnetostrictive case.</p>	<p>UNCLASSIFIED</p>	<p>UNCLASSIFIED</p>